Cell Stem Cell
Resource

Phosphorylation Dynamics during Early Differentiation of Human Embryonic Stem Cells

Dennis Van Hoof,[1,2,5,7] Javier Muñoz,[2,5] Stefan R. Braam,[1,3,5] Martijn W.H. Pinkse,[2,5,8] Rune Linding,[4,6] Albert J.R. Heck,[2,6,*] Christine L. Mummery,[1,3,6,*] and Jeroen Krijgsveld[2,6,9,*]

[1]Developmental Biology and Stem Cell Research, Hubrecht Institute, Uppsalalaan 8, 3584 CT Utrecht, The Netherlands
[2]Biomolecular Mass Spectrometry and Proteomics Group, Bijvoet Center for Biomolecular Research and Utrecht Institute for Pharmaceutical Sciences, Utrecht University, Padualaan 8, 3584 CH Utrecht, The Netherlands
[3]Department of Anatomy and Embryology, Leiden University Medical Center, Einthovenweg 20, 2333 ZC Leiden, The Netherlands
[4]Cellular & Molecular Logic Team, The Institute of Cancer Research (ICR), Section of Cell and Molecular Biology, 237 Fulham Road, SW3 6JB London, UK
[5]These authors contributed equally to this work
[6]These authors contributed equally to this work
[7]Present address: Diabetes Center, University of California, San Francisco, 513 Parnassus Avenue, San Francisco, CA 94143, USA
[8]Present address: Analytical Biotechnology Group, Delft University of Technology, Julianalaan 67, 2628 BC Delft, The Netherlands
[9]Present address: EMBL, Genome Biology Unit, Meyerhofstrasse 1, 69117 Heidelberg, Germany
*Correspondence: a.j.r.heck@uu.nl (A.J.R.H.), c.l.mummery@lumc.nl (C.L.M.), jeroen.krijgsveld@embl.de (J.K.)
DOI 10.1016/j.stem.2009.05.021

SUMMARY

Pluripotent stem cells self-renew indefinitely and possess characteristic protein-protein networks that remodel during differentiation. How this occurs is poorly understood. Using quantitative mass spectrometry, we analyzed the (phospho)proteome of human embryonic stem cells (hESCs) during differentiation induced by bone morphogenetic protein (BMP) and removal of hESC growth factors. Of 5222 proteins identified, 1399 were phosphorylated on 3067 residues. Approximately 50% of these phosphosites were regulated within 1 hr of differentiation induction, revealing a complex interplay of phosphorylation networks spanning different signaling pathways and kinase activities. Among the phosphorylated proteins was the pluripotency-associated protein SOX2, which was SUMOylated as a result of phosphorylation. Using the data to predict kinase-substrate relationships, we reconstructed the hESC kinome; CDK1/2 emerged as central in controlling self-renewal and lineage specification. The findings provide new insights into how hESCs exit the pluripotent state and present the hESC (phospho)proteome resource as a complement to existing pluripotency network databases.

INTRODUCTION

All future applications of pluripotent cells depend on exquisite control of their developmental fate. An essential first step for differentiation is exit from the pluripotent state, but exactly how this is regulated is unclear. Recent evidence for a core transcriptional machinery regulating pluripotency (Muller et al., 2008) has indicated the most important pathways for functional interrogation, but information on the activation state of component proteins is largely unknown. Here, we analyzed the proteome and phosphoproteome of human embryonic stem cells (hESCs), prototype pluripotent cells, for this purpose and compared this profile globally with that immediately after induction of differentiation.

ESCs are derived from preimplantation embryos, self-renew indefinitely, and can undergo multilineage differentiation (Thomson et al., 1998). Although mouse ESCs (mESCs) and hESCs have a similar core transcriptional regulatory network involving OCT4 (Niwa et al., 2000), SOX2 (Avilion et al., 2003; Yuan et al., 1995), and NANOG (Mitsui et al., 2003), they differ in their growth requirements. BMP and leukemia inhibitory factor sustain self-renewal of mESCs (Ying et al., 2003), but hESCs require basic fibroblast growth factor (bFGF) and transforming growth factor β (TGF-β)/Activin A signaling (Vallier et al., 2005; Xu et al., 2005). In fact, BMPs rapidly induce differentiation of hESCs (Pera et al., 2004; Xu et al., 2002). In all pluripotent cells, however, the pluripotent genes OCT4, SOX2, and NANOG collaborate by co-occupying the promoters of many genes, including their own, thereby promoting expression of ESC-associated genes and repressing lineage specification genes (Boyer et al., 2005; Loh et al., 2006).

Recent studies have shown that SOX2 can act synergistically with OCT4 in vitro to activate OCT-SOX enhancers and that SOX2 is necessary for regulating multiple transcription factors affecting OCT4 expression (Masui et al., 2007). Exactly how differentiating cells downregulate the transcription factors controlling self-renewal is unclear. Transcriptional regulation of NANOG by TGF-β/Activin A and BMP-responsive SMADs has recently been demonstrated. In undifferentiated hESCs, SMAD2/3 dominates through TGF-β signaling, whereas SMAD1/5/8 becomes activated upon BMP-induced differentiation. These SMADs bind the proximal promoter of NANOG with opposing effects; SMAD2/3 promotes but SMAD1/5/8 inhibits its expression (Xu et al., 2008). Furthermore, NANOG activity is regulated posttranslationally by caspase-mediated proteolytic cleavage, which is associated with differentiation (Fujita et al.,

2008). Although mESCs lacking NANOG are prone to differentiate, they still self-renew, suggesting that downregulation of NANOG alone is not sufficient to induce differentiation (Chambers et al., 2007).

Mass spectrometry (MS)-based proteomics is presently the most powerful tool for dissecting stimulus-dependent dynamics of phosphorylation events in living cells (Gruhler et al., 2005; Kratchmarova et al., 2005).We used stable isotope labeling by amino acids in cell culture (SILAC)-based quantitative MS (Ong et al., 2002) to study early phosphorylation and dephosphorylation events in hESCs upon BMP-induced differentiation. Metabolically labeled hESCs were compared quantitatively with unlabeled differentiating cells exposed for various times to BMP. TiO_2-based phosphopeptide enrichment followed by MS identified a large set of proteins phosphorylated in hESC, including SOX2. Mutational analysis suggested that phosphorylation of one or more consecutive serine residues induced SUMOylation. This posttranslational modification (PTM) has been described as inhibiting its transcriptional activity (Tsuruzoe et al., 2006). Using the NetworKIN algorithm (Linding et al., 2007), we linked the phosphorylation sites to their cognate kinases. This showed that, of the multiple active kinases, CDK1/2 had the largest number of substrates, including SOX2. Furthermore, comparison of cells before and after BMP exposure provided a global map of protein phosphorylation dynamics as hESCs exit the pluripotent state.

RESULTS

SILAC Analysis of hESCs and the Effect of BMP-Induced Differentiation

Undifferentiated hESCs were collected after 1 week of metabolic labeling with [$^{13}C_6$,$^{15}N_4$]-arginine and [$^{13}C_6$,$^{15}N_2$]-lysine (Figure 1). Rapid differentiation of unlabeled hESCs was induced by BMP4 addition in the absence of self-renewal growth factors (Pera et al., 2004); cells were harvested at various times thereafter (Figure 1). Western blot analysis shows that BMP4-induced differentiation, as previously, resulted in downregulation of OCT4 and SOX2 (Figure S1 available online). Phosphorylation dynamics were studied using an automated approach to enrich for phosphopeptides based on SCX and TiO_2 (Pinkse et al., 2008) combined with SILAC technology (Ong et al., 2002) for accurate relative quantitation. Proteins from undifferentiated hESCs (0 min) and differentiated cells (30, 60, and 240 min after BMP4 addition) were extracted, combined, and processed for quantitative MS analysis (Figure 1). MS intensities of the "light" and "heavy" peaks reflect the relative changes in protein phosphorylation between the two samples analyzed. Collectively, the three SILAC mixtures provided a four-time-point profile of phosphorylation events during early differentiation of hESCs (Figure 1).

The hESC Proteome and Phosphoproteome

From 800,000 spectra collected over 144 LC-MS/MS runs, 5222 proteins were identified with high confidence using a highly conservative Mascot Score of 35 at the peptide level (false discovery rate < 1%) (Tables S1 and S2). Because protein abundance cannot be predicted accurately from mRNA levels (Gygi et al., 1999), these data corroborated protein presence for many transcripts and additionally demonstrated the existence of proteins for which there was no direct evidence at the transcriptional level. Of the proteins identified, 1399 (27%) were phosphorylated on one or multiple residues (Figure S2, Table S3, and Data Set S1), making these proteome and phosphoproteome data sets the largest reported to date for hESCs. In total, 3090 unique phosphopeptides were detected, carrying 3067 phosphorylation sites localized on 2431 serines, 582 threonines, and 54 tyrosines. These proteome profiles represent a unique opportunity to gain insights into the functional protein content and identify active signaling pathways involving these proteins.

The proteins identified were first classified by molecular function, biological process, and subcellular localization (Figure S3). The two most abundant categories (molecular function) consisted of nucleic-acid-binding proteins (941 proteins, 18.0%) and transcription factors (343 proteins, 6.6%), suggesting that chromatin remodeling, modification, and transcription are highly active in hESCs. Gene ontology (GO) analyses confirmed enrichment of several GO terms related to these categories in our hESC proteome ($p < 0.001$, Hypergeometric test) (Table S4), compared to the entire human genome. To evaluate whether this overrepresentation was specific for pluripotent cells, we also classified two proteomes previously reported by our group (Van Hoof et al., 2006), hESCs (HES-2) and their differentiated derivatives (12 days in the absence of feeder cells) (Figure S4). Interestingly, we found a reduction ($p < 0.05$, chi-square test) in the abundance of transcription factors and nucleic acid binding as ESCs differentiated, indicating that this class of transcriptional and translational proteins is highly represented in ESCs. Next, we assessed whether proteins that were identified originated from genomic regions predicted to be active, as indicated by K4 trimethylation of histone 3 (H3K4me3), or silent, marked by trimethylation on K27 (H3K27me3) (Barski et al., 2007; Mikkelsen et al., 2007). Our proteome notably correlated with whole-genome analysis of histone 3 methylation in hESCs (Pan et al., 2007), given that 2848 proteins in our catalog carried the activating H3K4me3 mark on their corresponding genes, 279 proteins had both H3K4me3 and H3K27me3 marks, and 240 proteins had neither H3K4me3 nor H3K27me3, whereas only 9 were reported as silenced genes (Figure S5 and Table S5).

Phosphorylation Dynamics during Differentiation

Of the 3090 unique phosphopeptides identified, 1987 were quantified in at least one of the three SILAC mixtures (Figure S6, Table S3, and Data Set S1).We achieved a relative standard deviation (RSD) of 7% (data not shown) by measuring modified variants of the reported phosphopeptides resulting from trypsin missed cleavages or methionine oxidations. On this basis, we found that 1091 phosphopeptides (50% of the quantified phosphoproteome) were regulated during differentiation (Table S3 and Data Set S1). Next, we examined the relationship between peptide abundance and its regulation status (i.e., differentially regulated or not), applying total peptide count (including multiple observations of the same peptide within a single experiment). We observed an inverse correlation between frequency and regulation status (Figure S6B), indicating that low-abundant peptides tended to be more regulated than high-abundant peptides. Thirty minutes after BMP4 addition, the level of phosphorylation of 407 proteins was increased, whereas only 25 decreased. Changes of similar magnitude were found at

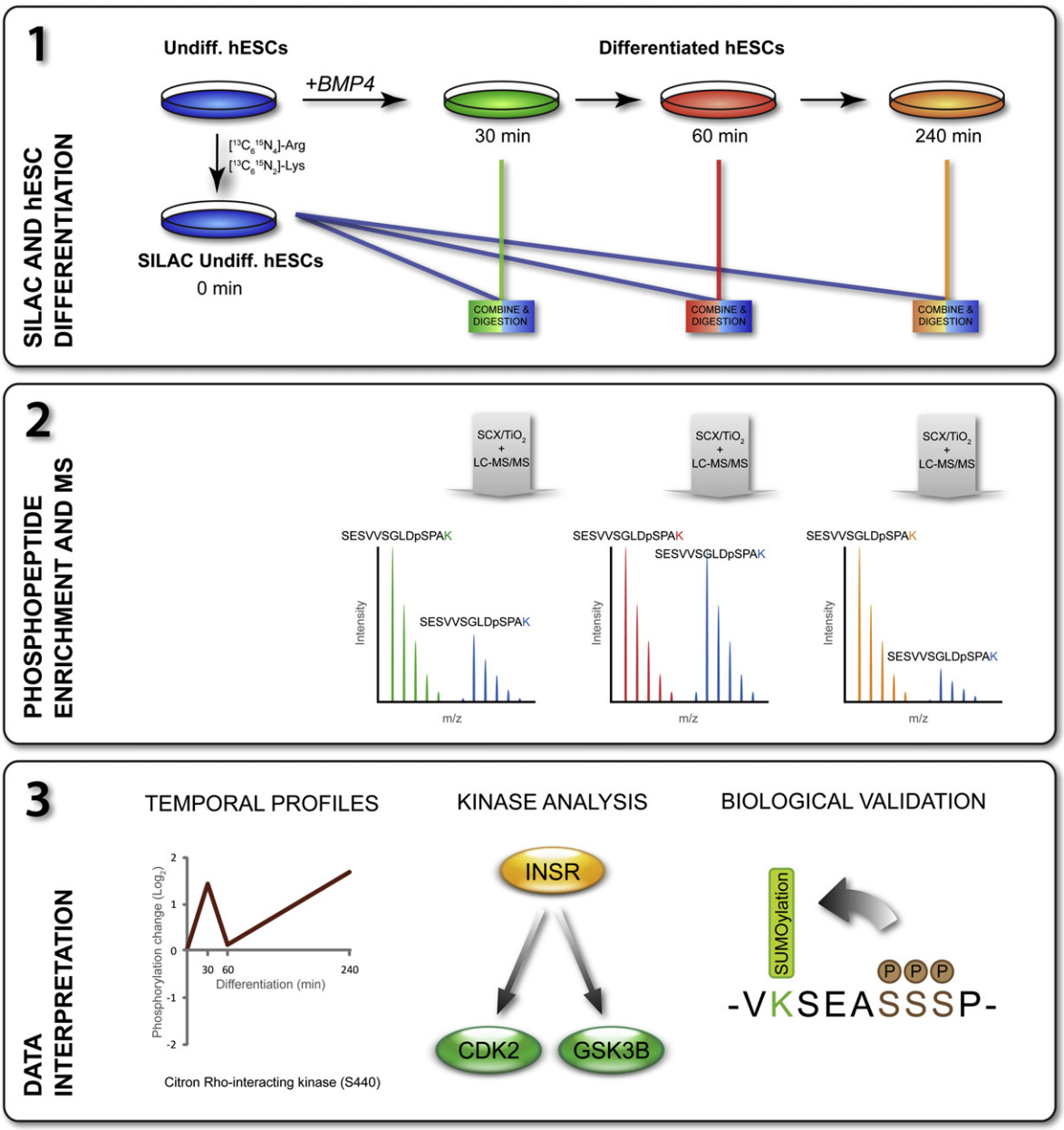

Figure 1. Experimental Design

(A) Two populations of hESCs were used, one labeled with SILAC amino acids [$^{13}C_6$,$^{15}N_4$]-arginine and [$^{13}C_6$,$^{15}N_2$]-lysine. Differentiation of unlabeled hESCs was induced by BMP4, and samples were collected at 30, 60, and 240 min. Differentiated cells and SILAC-labeled hESCs were combined, lysed, and enzymatically digested.

(B) The three mixtures were subjected to phosphopeptide enrichment based on TiO_2 and SCX prior to high-resolution LC-MS/MS analysis. The peak intensities of the identified phosphopeptides are proportional to their relative abundance.

(C) The three SILAC mixtures provide a profile of phosphorylation events over four time points after the onset of differentiation. Phosphorylation networks were reconstructed by predicting potential kinases for every phosphosite identified. SUMOylation of the pluripotency transcription factor SOX2 was found to be phosphorylation dependent.

60 min (506 upregulated, 51 downregulated) and 240 min (622 upregulated, 42 downregulated), suggesting an overall increase in kinase activity. The time course showed a trend in most of the phosphopeptide profiles, showing up- or downregulation at minimally two consecutive time points, suggesting the robustness of the data set. Second, we confirmed phosphorylation profiles for GSK3β and 4EIFEBP1 by immunofluorescence and western blotting, the method of choice being dictated by the properties of available antibodies (Figure S10).

To gain insight into temporal regulation during differentiation, phosphopeptides quantified at all time points and significantly differing in phosphorylation in at least one of the four time points

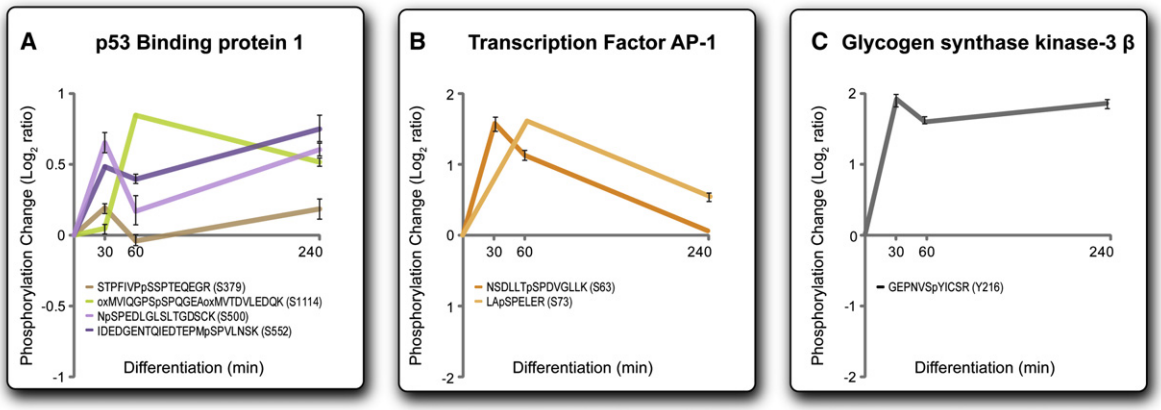

Figure 2. Temporal Profiles of Phosphorylation during Differentiation

Changes in phosphorylation levels are shown for those proteins cited in the text.

(A) Specific regulation of four different phosphorylation sites from TP53BP1. S1114 shows a delayed phosphorylation, whereas S500 and S552 belong to intermittent profile. S379 is not regulated during differentiation.

(B) Two phosphopeptides were identified for AP-1 (c-Jun), both of which were transiently phosphorylated.

(C) Y216 from GSK3B shows a sustained phosphorylation profile.

Error bars are shown if the phosphopeptide was quantified more than two times. See Figure S10 for confirmatory western blot and immunofluorescence analyses.

were grouped by k-means clustering (Figure S7 and Table S6). Two phenomena become apparent from these data. First, the most dramatic phosphorylation changes took place during the first hour, coincident with SMAD1/5/8 phosphorylation in hESC (Pera et al., 2004). No phosphopeptides were regulated after 4 hr only, indicating that events are initiated by BMP4 within this time frame. Second, apart from a small group of dephosphorylation events (cluster ''dephosphorylation'' in Figure S7), most changes represent an increase in phosphorylation level. In several cases, the same proteins occupied more than one cluster, indicating that regulation of phosphorylation is site specific and that individual sites may be affiliated with different functions. This is congruent with the idea that proteins can serve as platforms for integrating signals from various kinases/cascades (Olsen et al., 2006). One example is tumor suppressor p53-binding protein 1 (TP53BP1), a hyperphosphorylated transcription activator engaged in the response to DNA damage (Botuyan et al., 2006), checkpoint signaling during mitosis (Swiss-Prot by similarity), and hESC differentiation (Pan et al., 2007). Three phosphopeptides identified for TP53BP1 were regulated with different kinetics because they belonged to different profile clusters (delayed and intermittent) (Figure 2 and Table S6).

Signaling Pathways Activated upon BMP-Induced Differentiation

The coverage of signaling pathways was assessed by projecting protein identification and quantitative phosphorylation on 130 signaling pathways in Panther (Mi et al., 2007). Components of nearly all pathways were represented in our data (Figures 3A and S8), 86 of which contained between 1 and 79 phosphorylated proteins. Seventy pathways were represented by proteins with dynamic phosphorylation (Table S7). This suggests activation of a protein network composed of multiple signaling cascades. To investigate this in greater detail, we considered key components of individual pathways and looked at whether the observed phosphorylation sites were those known to be involved in protein activation. Activation of the BMP pathway was indicated by phosphorylation of receptor SMADs, SMAD5 and SMAD8 at S465 and S467, respectively, confirming activation of the BMP4-SMAD-signaling cascade in hESCs (Figures S9A and S9B) as described previously (Pera et al., 2004).

Several components of PI3K signaling were identified (Figures 3 and S10). Increased phosphorylation of PDPK1 at S241 indicated activation of this kinase for subsequent phosphorylation of its target AKT1 (PKB). Additionally, an increase in phosphorylation of various proteins with confirmed AKT1 target sites was observed, including S166 of MDM2, S280 of CHK1 (both of which lead to inhibition of p53-mediated apoptosis), and S341 and S588 of TBC1D4 (also known as AS160). These all point to activation of AKT1.

c-Jun, which forms the heterodimeric activator protein 1 transcription factor complex with c-Fos, was phosphorylated at S63 and S73, suggesting activation of the JNK pathway. Interestingly, the immediate phosphorylation of c-Jun after differentiation induction at 30 min was followed by a decrease over the next hours (Figure 2B), indicating that JNK activation was transient. Wnt signaling is one of the best-covered pathways in our data set and included multiple proteins with phosphorylation changes (Figure S9C). Among these was an activating phosphorylation at Y216 of GSK3B that was induced within 30 min of BMP addition (Figure 2C). Phosphorylation of this tyrosine over time was confirmed in a biological repeat on cell lysates using western blotting and at the single-cell level using immunofluorescent antibody staining (Figure S10). Furthermore, several peptides of the key Wnt-signaling protein, β-catenin, were identified. However, the N-terminal phosphopeptide-marking activity was not detected, so the activation status of β-catenin could not be determined from our data directly. However, several coactivators (BCL9, BCL9L, PYGO2) and repressors (TLE1, TLE3) (Chen and Courey, 2000) of β-catenin were differentially phosphorylated at several positions, indicating some level of

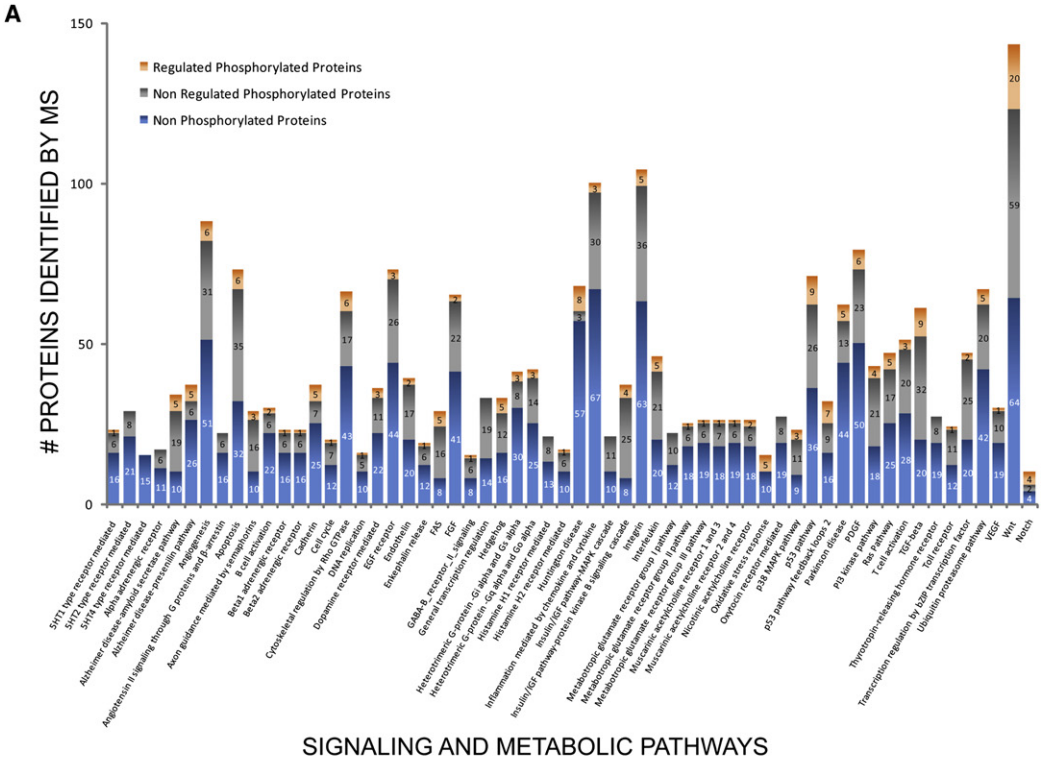
A
PROTEINS IDENTIFIED BY MS
Regulated Phosphorylated Proteins
Non Regulated Phosphorylated Proteins
Non Phosphorylated Proteins
SIGNALING AND METABOLIC PATHWAYS

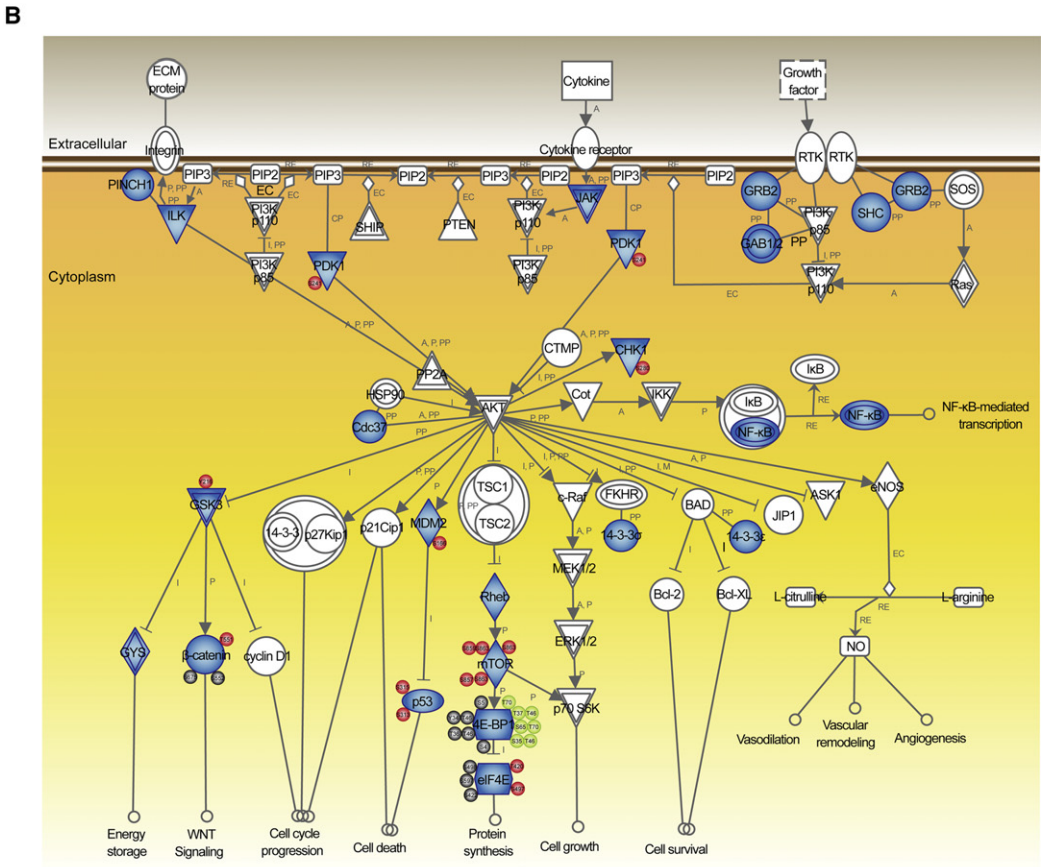
B
Extracellular
Cytoplasm
ECM protein
Integrin
Cytokine
Cytokine receptor
Growth factor
RTK
PINCH1
ILK
PIP3
PIP2
PI3K p110
PI3K p85
SHIP
PTEN
JAK
PDK1
GRB2
GAB1/2
SHC
SOS
Ras
CTMP
CHK1
PP2A
HSP90
Cdc37
AKT
Cot
IKK
IkB
NF-kB
NF-kB-mediated transcription
GSK3
14-3-3
p27Kip1
p21Cip1
MDM2
TSC1
TSC2
c-Raf
FKHR
BAD
JIP1
ASK1
eNOS
MEK1/2
ERK1/2
Rheb
mTOR
p53
4E-BP1
eIF4E
p70 S6K
Bcl-2
Bcl-XL
L-citrulline
L-arginine
NO
Vasodilation
Vascular remodeling
Angiogenesis
SYS
β-catenin
cyclin D1
Energy storage
WNT Signaling
Cell cycle progression
Cell death
Protein synthesis
Cell growth
Cell survival

Table 1. hESC Markers and Phosphorylation Sites Identified

IPI Number	Gene Symbol (Protein Name)	Phosphosites Identified
IPI00002948	LIN28 (Lin-28 homolog A)	S3[a], S200, T202
IPI00012593	DNMT3B (isoform 1 of DNA (cytosine-5)-methyltransferase 3B)	S82[a], S136, S202, S209[a], T383, S387
IPI00300620	IFITM1 (interferon-induced transmembrane protein 1)	
IPI00219089	POU5F1 (isoform A of POU domain, class 5, transcription factor 1; OCT4)	
IPI00009703	SOX2 (transcription factor SOX2)	S249, S250, S251
IPI00026637	GAL (Galanin precursor)	S116[a]
IPI00020668	UTF (undifferentiated embryonic cell transcription factor 1)	S18, T35[a], S245[a]
IPI00007164	FOXD3 (forkhead box protein D3)	
IPI00299659	GDF3 (growth/differentiation factor 3 precursor)	
IPI00045497	NODAL (nodal homolog precursor)	
IPI00299116	PDXL (Podocalyxin-like protein 1 precursor)	
IPI00434539	NANOG (isoform 1 of Homeobox protein NANOG)	

[a] These phosphosites were found to be regulated during the differentiation process.

regulation of Wnt signaling. Moreover, phosphorylation of casein kinase I, which phosphorylates β-catenin, was increased on at least two sites. Combined, these data implied rapid activation of the Wnt pathway at the onset of BMP-induced differentiation.

Many other phosphorylation events were also observed, but their effects on the activation of proteins affected are largely unknown. Nonetheless, their multitude and diversity, as well as the fact that some of them are shared by several pathways (e.g., G3BP1 and G3BP2) (Irvine et al., 2004) indicated that induction of differentiation initiates signaling via an intricate network that vigorously alters the behavior of hESC.

Additional Effects of Differentiation Induction

To investigate the effects of BMP4-induced differentiation beyond kinase signaling, proteins with altered phosphorylation levels (> 0.5-fold, $\log_2$ scale) were mapped to GO terms with respect to molecular function (Table S8) and biological process (Table S9). These analyses showed the broad range of protein classes affected by differentiation, indicating that its effects extended well beyond those proteins participating in established signal transduction cascades. Some of the processes are related directly to differentiation itself (e.g., alteration of cell-cycle kinetics or cell-cycle exit and initiation of germ layer specification); however, it was unclear exactly how the individual components were affected. To address this, the same set of phosphoproteins was subjected to an unbiased analysis using Anni (Jelier et al., 2008), an ontology-based interface that applies text mining to retrieve associations between proteins by co-occurrence in the literature. This tool classifies proteins by a term or "concept" that they have in common, which is not necessarily a GO term. Although some of the 39 clusters identified in this manner (Figure S11 and Table S10) were also defined by GO analysis (e.g., cell-cycle, cytoskeleton), many additional concepts emerged, such as transcriptional repression, transcriptional elongation factors, translation initiation factors, and SWI/SNF chromatin remodeling (Jaenisch and Young, 2008). This implies that established mechanisms associated with differentiation, like genome remodeling, silencing of the pluripotency network, and activation of differentiation-inducing genes, are initiated rapidly after induction. Additionally, the presence of a protein SUMOylation cluster indicated active posttranslational processing of proteins. Furthermore, clusters containing Rab11 family-interacting proteins, microtubule associated proteins, vimentin, GTPase-activating proteins, tight junction proteins, and focal adhesion proteins strongly suggested remodeling of the cellular matrix.

Phosphorylation of Pluripotency-Associated Proteins

To determine the phosphorylation status of proteins associated with pluripotency, we mapped MS identifications to ESC-associated genes defined by the International Stem Cell Initiative (Adewumi et al., 2007). From the top 20 genes with a NANOG pairwise correlation coefficient > 0.5, we detected the protein products of 12, including the three core transcription factors OCT4, SOX2, and NANOG (Table 1). Sixteen novel phosphosites were identified in five of these proteins; among these were three residues of UTF1, three residues of LIN28, seven residues of DNMT3B, and three consecutive residues of SOX2. During differentiation, the phosphorylation state changed for six of the sites identified, suggesting that the ESC-associated proteins to which they belong are regulated posttranslationally. To find differential phosphorylation sites of downstream targets for OCT4, SOX2, and NANOG, we mapped the phosphoproteomes to chromatin immunoprecipitation data sets published for OCT4, SOX2, and NANOG (Boyer et al., 2005). Of the 2260 genes reported, we found 586 products, 100 of which were phosphoproteins regulated during differentiation, including 19 transcriptional regulators (Figure 4 and Table S11). Interestingly, these phosphorylated proteins are predominantly components of the RNA posttranscriptional modification (e.g., SFPQ, DDX20, ADAR, ACIN1, SFRS7) and the gene expression machinery (e.g.,

Figure 3. Signaling Pathways Analysis

(A) Nonphosphorylated proteins, nonregulated phosphoproteins, and regulated phosphoproteins were mapped to 130 pathways with Panther classification system (Mi et al., 2007). Only those pathways with a relative high coverage are shown. The complete analysis can be found in Table S7 and Figure S8.

(B) Graphical representation of PI3K/AKT-signaling pathway. Identified proteins by MS are represented in blue color. Identified phosphosites are also shown when applicable (red, upregulated site; green, downregulated; gray, not regulated or not quantified). Some examples of other pathways can be found in Figure S9.

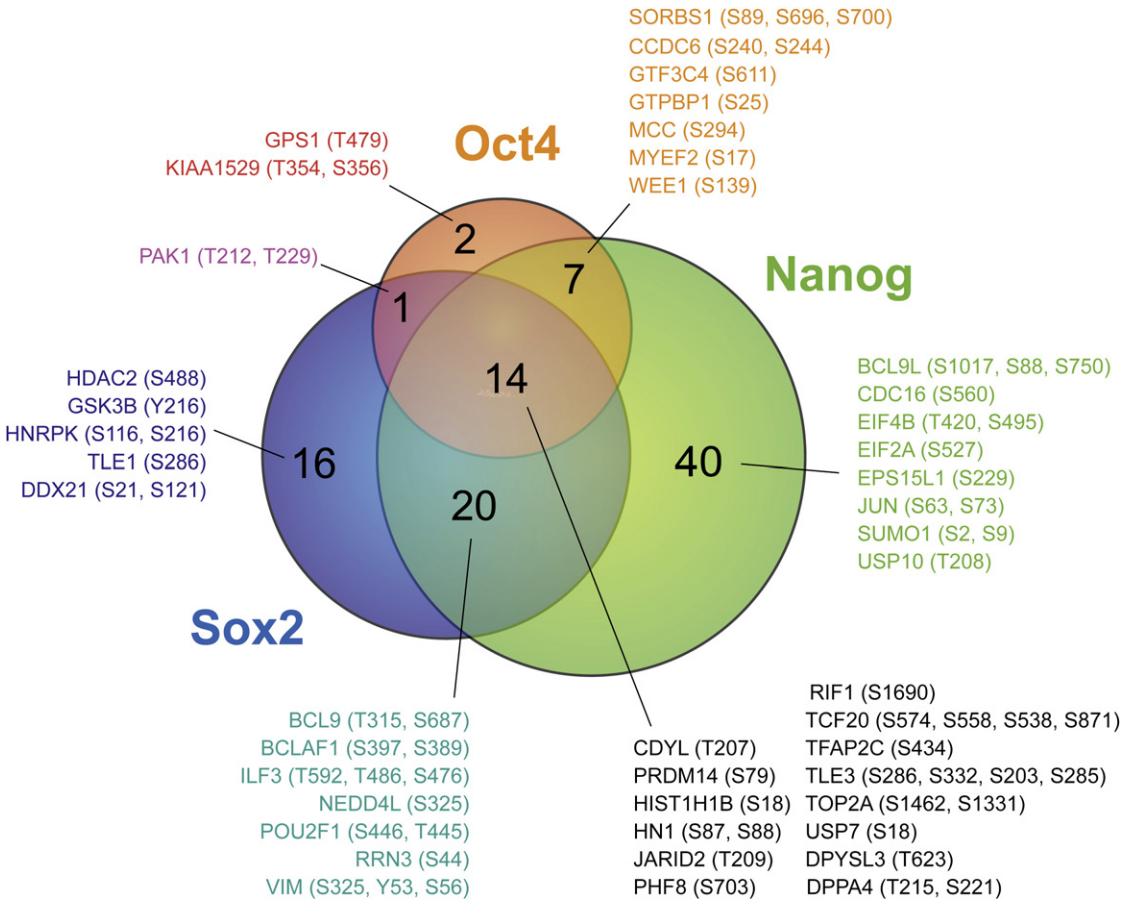

Figure 4. Downstream Targets of the Core Transcriptional Regulatory Circuitry Regulated by Phosphorylation

Venn diagram representing the overlap of OCT4, SOX2, and NANOG target genes differentially phosphorylated during differentiation. Examples of regulated phosphosites are shown for every section of the diagram. The full list of proteins can be found in Table S11.

POU2F1, SFPQ, PAK1, STAT3, SUMO1, SOX2, HIST1H1). These results suggested that many components of the hESC core transcriptional circuitry are regulated by phosphorylation and that differentiation is accompanied by active modulation of these processes.

Phosphorylation-Dependent SUMOylation of SOX2

Our MS results showed that SOX2 can be phosphorylated at three consecutive serine residues: S249, S250, and S251 (Table S3 and Data Set S1). This serine triplet flanks an upstream SUMOylation site of SOX2 (Tsuruzoe et al., 2006), the combination of which resembles the phosphorylation-dependent SUMOylation motif (PDSM), ΨKxExxSP, described in other SOX family members (Hietakangas et al., 2006). We hypothesized that SUMOylation of SOX2 depends on phosphorylation of one or more of these serine residues in a similar manner. To address whether crosstalk occurs between these phosphorylation and SUMOylation sites, a set of SOX2 mutants was created, and their SUMOylation state was investigated using HeLa cells stably expressing SUMO2 (Vertegaal et al., 2006) (Figures 5, S12A, and S12B). Expression of WT human SOX2 in these cells showed a low basal level of SUMOylated SOX2 compared with free SOX2 (Figures 5 and S12B). However, when the serine residues were replaced by aspartic acid ($SOX2_{S249–251D}$) to mimic constitutive phosphorylation, high levels of the SUMOylated SOX2 mutant were observed, including double- and triple-SUMOylated forms (Figures 5 and S12B). On the other hand, replacing the serine residues by alanine ($SOX2_{S249–251A}$) showed a ratio between the free and SUMOylated form similar to that of WT SOX2 (Figures 5 and S12B). Furthermore, replacing K245 of the PDSM by alanine ($SOX2_{K245A}$) completely prevented SUMOylation of the transcription factor (Figure S12B), indicating that this lysine residue is the only target for SUMOylation under these conditions. Notably, none of these mutations affected the nuclear localization of SOX2 in HUES-7 cells (Figure S12C), which suggested that phosphorylation of these serine residues did not initiate immediate export of SOX2 from the nucleus.

The hESC Kinome Network

Consensus motifs of phosphorylation sites are inappropriate for systematic matching with their corresponding kinases, as specificity is largely determined by context (Linding et al., 2007). Linding et al. addressed this issue by developing an algorithm (NetworKIN) that introduces the concept of combining probabilistic modeled network context with linear motifs recognized by the catalytic domain of kinases (Linding et al., 2007).

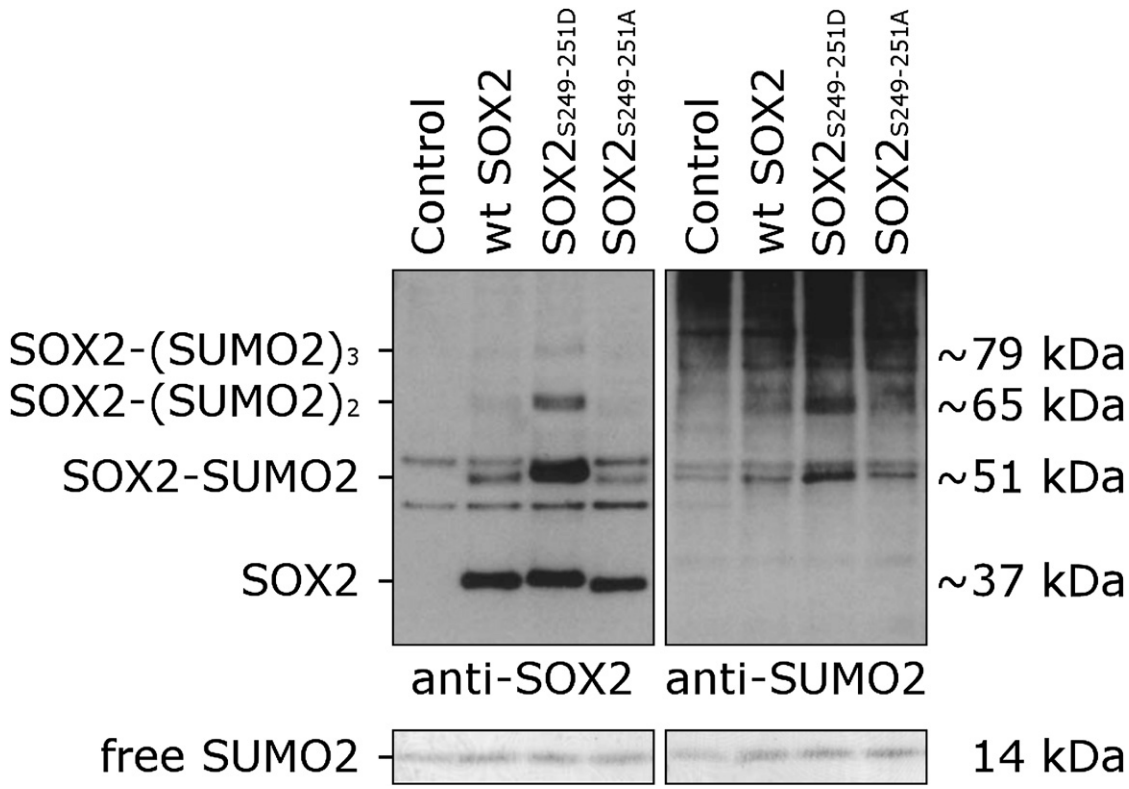

Figure 5. Phosphorylation-Dependent SUMOylation of SOX2

HeLa cells stably expressing His_6-SUMO2 ($HeLa^{SUMO2}$) were transfected with pCAG expression constructs harboring either GFP (Control), WT Sox2, $Sox2_{S249–251D}$, or $Sox2_{S249–251A}$. Cells were lysed, and His_6-SUMO2 conjugates were enriched on nickel-nitrilotriacetic acid-agarose beads. Purified fractions were subjected to SDS-PAGE and immunoblotted using antibodies to detect Sox2 or SUMO2/3. These results indicate that SUMOylation of SOX2 depends on phosphorylation at S249–251.

Relationships between kinases and all of the phosphorylation sites defined here were predicted, creating, for the first time, a kinase-substrate database for hESCs (Table S12). This was used to create an in vivo kinome for hESCs (Figure 6A), comprising 107 kinases, representing most of the known kinase families (Manning et al., 2002). Interestingly, CDK1/2 appeared to play a prominent role, given that it was predicted to phosphorylate ~1200 peptides in our assay. To investigate this further, all kinases were predicted for Phospho.ELM (Diella et al., 2004) and PhosphoSite (http://www.phosphosite.org), two publicly available repositories of human phosphorylation sites, with > 23,000 unique phosphosites. By comparing this hypothetical absolute kinome with the hESC-specific kinome, kinases that are under- or overrepresented in hESCs, based on the incidence of specific phosphorylations, could be identified (Figure S13). For instance, CDK1/2 was found to mediate 26% of the phosphorylation events in hESCs, which is significantly more ($p < 0.0001$, chi-square test) than the 12% of all theoretical phosphorylation sites in humans. Additional kinases with activities overrepresented in hESCs were MAPK8, MAPK11, MAPK14, TGFBR2, GSK3B, and NEK2, the latter being a known modulator of the cell cycle, just as CDK1/2. Furthermore, CDK1/2, NEK2, and GSK3B are potential effectors of SOX2 phosphorylation (Table S12). These findings suggest that prevalent kinases control cell-cycle processes as well as the activity of pluripotency-associated transcription factors, both of which are characteristic of ESCs. The MS data indicated that CDK2 is phosphorylated progressively at Y15, marking a decrease in its activity (Gu et al., 1992). Linking site-specific kinases that were found regulated over the investigated time course with their corresponding upstream kinases generated a temporal kinase-cascade model that illustrates the dynamics in kinase relationships during differentiation (Figure 6B). This overview suggested that the initial signal that disturbs the ESC-associated network expands over time by activating an increasing number of kinases, resembling the model proposed previously (Miller-Jensen et al., 2007).

DISCUSSION

Self-renewal in pluripotent hESCs is highly sensitive to factors that trigger differentiation through transmission of signals to the nucleus. Activation and inactivation of intracellular proteins by phosphorylation and dephosphorylation are among the earliest events following binding of a ligand to its receptor. In addition to regulating protein activity, phosphorylation also contributes to controlling cell identity by fine-tuning protein expression. We used MS-based quantitative proteomics here to monitor dynamic changes in the phosphoproteome of hESCs at the onset of BMP4-induced differentiation. We probed the hESC proteome to a depth of 5222 proteins, 586 of which are

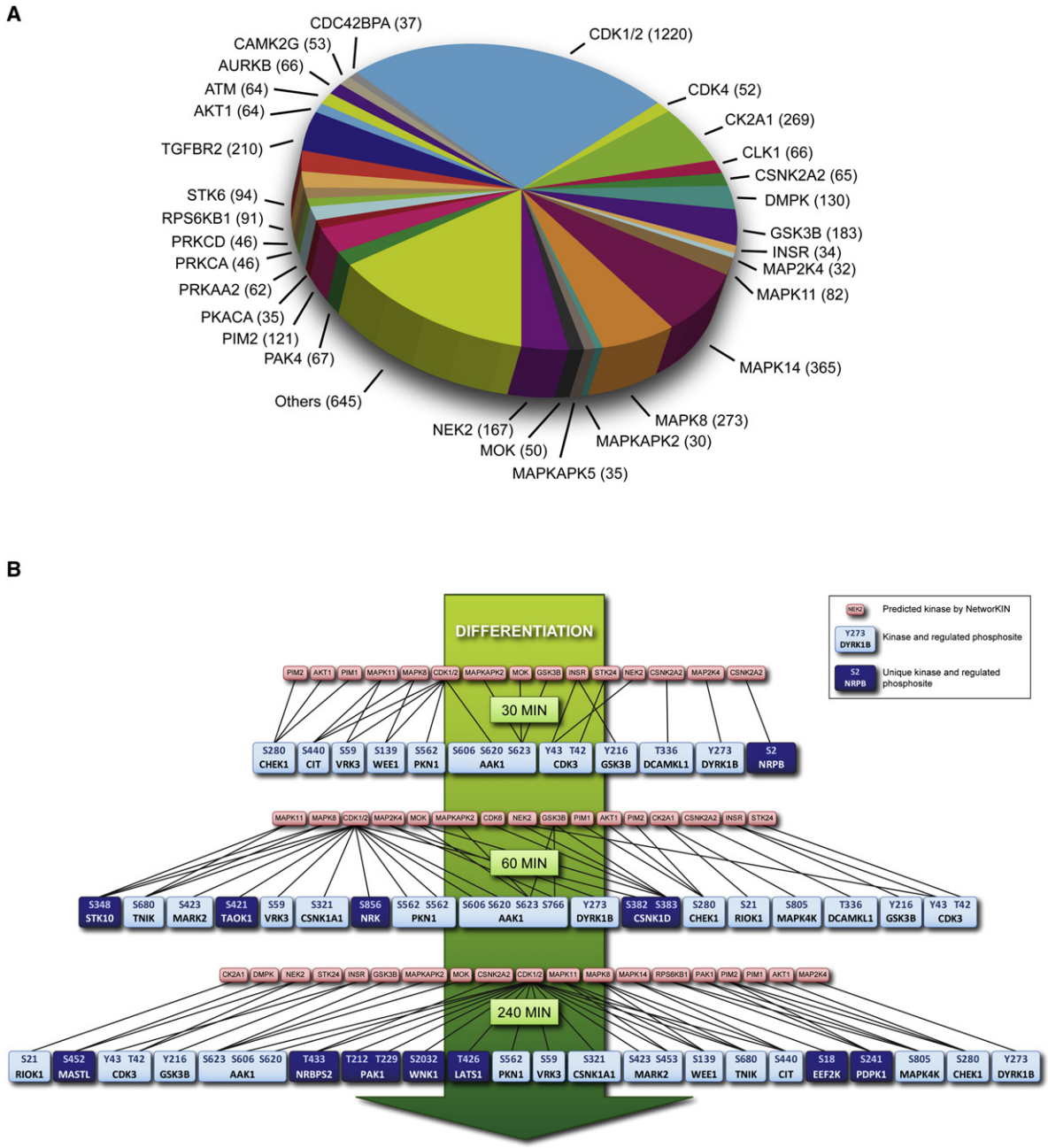

Figure 6. Phosphorylation Networks during hESC Differentiation

The NetworKIN algorithm was used to predict kinases for every phosphorylation site identified.

(A) In total, 107 kinases were predicted to regulate the hESC phosphoproteome; the number of substrates is indicated in the pie chart. Kinases predicted to phosphorylate < 30 substrates are shown combined in "others."

(B) By linking regulated kinases (blue boxes) to their predicted upstream kinases (red boxes), kinase cascades during hESC differentiation were modeled. Kinases regulated at only one time point are depicted as dark blue boxes. This illustrates how a signal spreads over time.

thought to be regulated by the core transcriptional network. Because this core transcriptional network was postulated on the basis of ChIP data and transcription factor binding does not necessarily mean that the particular gene is regulated by that factor, our data set provides high-quality confirmation of the involvement of many proposed players. GO annotation of the hESC proteome resulted in prominent subclasses consisting of proteins associated with epigenetic modification (Pan et al., 2007), transcription (Boyer et al., 2005; Efroni et al., 2008), and translation (Sampath et al., 2008), suggesting that these processes are prominent in hESCs. Among the 1399 proteins phosphorylated on a total of 3067 residues, more than 1200 sites had not been reported previously to our knowledge, 430 belonging to the class of proteins that participate in the core

transcriptional regulatory circuitry (Boyer et al., 2005). This implies that the activity of many proteins involved in the pluripotency and self-renewal network is regulated by a selection of kinases and phosphatases.

Interruption of self-renewal by exogenous factors has major effects on signaling networks that sustain the undifferentiated state. Changing the identity of hESC by exposure to extracellular stimuli is immediately followed by a complete reconstitution of signaling pathways. This was exemplified by the observation that half of the phosphoproteome was modulated within the first hour of BMP4 exposure. In addition to the expected phosphorylation of receptor SMADs, increased phosphorylation of several substrates of AKT1 were detected, indicating activation of the PI3K/AKT pathway. This might have resulted from signaling through the insulin receptor (Freund et al., 2008), as hESC differentiated in medium containing insulin as a survival factor. In addition, S63 and S73 of c-Jun were phosphorylated, though temporarily, suggesting transient activity of JNKs. Although crosstalk between intracellular pathways cannot be deduced from the present data, there is evidence for reciprocal interactions between JNKs and AKT. JNKs can phosphorylate AKT1 at T450, thus priming this protein for activation through phosphorylation by PDK1 (Shao et al., 2006). Conversely, AKT1 can inhibit the JNK pathway by phosphorylating ASK1 (MAPKKK5), which lies upstream of JNKs. This apparent dichotomy is in agreement with our data, as phosphorylation of c-Jun was early and transient, whereas phosphorylation of AKT substrates was sustained. This would tip the balance of proapoptotic (JNKs) and antiapoptotic signaling (AKT) in favor of the latter.

In addition to changes in signaling pathways, we also found alterations in established and proposed regulators of pluripotency. For instance, a novel acetylation and three novel phosphorylation sites on LIN28 were identified. Ectopic expression of LIN28 contributes to formation of iPSCs, illustrating the importance of this pathway in regulating the pluripotent state (Yu et al., 2007). Furthermore, LIN28 is known to block maturation of primary pri-Let-7g transcripts to mature Let-7g transcripts (Viswanathan et al., 2008). This led to the hypothesis that Let-7 and LIN28 participate in an incoherent feed-forward loop that contributes to rapid differentiation (Marson et al., 2008). Another example is the detection of three novel phosphorylation sites on the transcription factor UTF1, a chromatin-associated transcriptional repressor crucial for differentiation of mESCs (van den Boom et al., 2007); two of the phosphorylation sites were regulated upon differentiation. For DNMT3B, six novel phosphorylation sites were identified, two of which were regulated. Upon differentiation, methyltransferases DNMT3A and DNMT3B are recruited to the OCT4 promoter, thereby repressing its transcription through CpG methylation (Feldman et al., 2006). We also identified three novel consecutive phosphosites on SOX2, which we investigated in more depth.

The transcription factor SOX2 is one of the three core transcription factors that play essential roles in embryonic development (Avilion et al., 2003; Yuan et al., 1995) and self-renewal of ESCs (Fong et al., 2008; Masui et al., 2007). However, little is known about how the activity of SOX2 itself is regulated. Whereas SUMO conjugation was found to inhibit binding of mouse SOX2 to DNA (Tsuruzoe et al., 2006), the PDSM defined initially in SOX3, SOX8, and SOX9, among other transcriptional regulators, had not been identified in SOX2 (Hietakangas et al., 2006). This can be explained by a surplus residue between E247 and S251, which does not match the established consensus sequence (Hietakangas et al., 2006). Combined, our findings indicated that the consensus of this PDSM is rather flexible and suggested that the three adjacent serine residues immediately upstream of P252 have redundant functions. Moreover, they imply that transcriptional activity of SOX2 is regulated by SUMOylation that results from phosphorylation. Interestingly, all phosphorylated forms of SOX2 were identified in hESCs, but none increased significantly upon differentiation, suggesting that transcriptional activity of SOX2 is controlled stringently both in differentiating and undifferentiated ESCs. A critical level of functional SOX2, essential for self-renewal (Chew et al., 2005; Kopp et al., 2008), is probably maintained by a fine balance between de novo synthesis, PTMs that alter its activity, and translocation from the nucleus followed by degradation. Of note is that all SOX2 mutants were localized predominantly in the nuclei of HUES-7 transfectants. This implies that phosphorylation of SOX2, as mimicked by the S249-251D mutation, and the consequent SUMOylation at K245 do not immediately lead to massive nuclear export and subsequent targeting for degradation. Presumably, the SUMOylation pathway is saturated when SOX2 is overexpressed in HUES-7 cells, requiring concomitant overexpression of SUMO in order to detect SUMOylated forms of SOX2, as observed for SUMO2-overexpressing HeLa cells. Further investigation is needed to determine the balance between de novo synthesis and degradation of SOX2 and the role of PTMs therein.

Using the NetworKIN algorithm to predict the kinases responsible for phosphorylation during differentiation, we reconstructed a hESC kinome composed of 107 kinases, 26 of which were regulated by phosphorylation upon induction of differentiation. Because of their low abundance, only 54 phosphotyrosine peptides were identified; consequently, receptor Tyr kinases (e.g., INSR, EPHA4, and IGFIR) seem underrepresented. In contrast, 2431 phosphoserine peptides were identified, pointing to a central role for CDK1/2. In addition to CDK1/2 and GSK3B, MAPK8 (a JNK protein), as well as MAPK11 and MAPK14 (p38 MAPK proteins) of the CMGC Ser/Thr protein kinase family (Manning et al., 2002), have well-documented functions in differentiation. p38 MAPKs are inhibitory during cell commitment and are antiapoptotic during late stages of differentiation, whereas the proapoptotic JNKs are involved in ectoderm and primitive endoderm differentiation (Binetruy et al., 2007). However, protein phosphorylation is regulated by a precise control of protein kinase (PK) and protein phosphatase (PP) activities. PPs are regulated, in the same way as kinases, by an array of targeting and regulatory subunits, PTMs, and by specific inhibitors. A total of 43 PPs (30% of all phosphatases reported in SwissProt) were identified in our data set; four of them presented differentially regulated phosphosites: PPMH1 (Ser/Thr PPs), DUSP19 (dual specificity PPs), and PTPN13 and PTPN14 (Tyr PPs). PKs, as well as PPs, possess basal activities; therefore, it should be noted that some of the upregulated phosphopeptides in our study could result from inhibition of their specific PPs, rather than from an increase of the kinase activity. The same applies for downregulated phosphopeptides.

It is not surprising that most dynamic phosphorylation of signaling cascade components occurred within 30 min of

BMP4 exposure, given that similar kinetics had been observed by others studying EGF stimulation in HeLa cells (Olsen et al., 2006). The multiplicity of components of the network in hESCs and their initiation upon differentiation are far too complex to be covered in entirety here. Nevertheless, the multitude and variety of proteins that undergo phosphorylation changes during the first hours of differentiation suggest rapid and dramatic reorganization of the proteome that extends far beyond signaling alone. Proteins affected were classified based on GO annotation and contextual co-occurrence in literature. These included methylation, transcription initiation, and transcriptional elongation, indicating that silent developmental genes controlled by OCT4, SOX2, and NANOG experience complex transcriptional regulation (Guenther et al., 2007). These genes are occupied by nucleosomes with histone H3K4me3 and histone H3K27me3. Although transcription is initiated, there is no productive elongation because of repression by PcG proteins (Azuara et al., 2006; Bernstein et al., 2006). Transcriptional repression of ESC-associated genes and SWI/SNF chromatin remodeling are also concepts associated with differentiation. Furthermore, the emergence of a protein SUMOylation cluster (consisting of E3 ligases, hydrolase, and SUMO-isopeptidase) suggests that this type of PTM is a concept linked to differentiation that extends beyond the effects on SOX2 described above. Finally, the presence of clusters containing Rab11 family-interacting proteins, microtubule-associated proteins, vimentin, GTPase-activating proteins, tight junction proteins, and focal adhesion proteins suggested that initiation of differentiation leads to remodeling of cell shape. We had shown previously that hESCs grown as monolayer cultures under feeder-free conditions (i.e., identical to those used in this study) have an epithelial phenotype, evidenced by the expression of proteins belonging to adherence junctions, tight junctions, gap junctions, and desmosomes (Van Hoof et al., 2008). The observation that proteins forming these structures undergo increased phosphorylation strongly suggests that their biogenesis changes (Eckert and Fleming, 2008) during a process that is initiated at the onset of differentiation.

Conclusions

In addition to an extensive profile of the hESC proteome, our approach generated a dynamic map of protein phosphorylation during differentiation of hESC showing concordance over time, which we used to define a wide spectrum of novel kinase substrates. These data provide a rich resource for further investigation of the function of individual proteins, as exemplified by the phosphorylation sites of SOX2 that regulate its transcriptional activity through SUMOylation. Linking genomic, epigenomic, transcriptomic, and proteomic approaches will improve our knowledge of stem cell biology and (human) development and, thereby, our ability to control self-renewal versus differentiation fate decisions by pluripotent cells.

EXPERIMENTAL PROCEDURES

SILAC Labeling of hESCs and Differentiation

HUES-7 hESCs were cultured, as previously (Braam et al., 2008), on Matrigel without MEFs and differentiation induced by 50 ng/ml of BMP4. For details, see Supplemental Experimental Procedures.

Western Blotting

Western blotting was carried out as previously (Van Hoof et al., 2006). For details, see Supplemental Experimental Procedures.

Phosphopeptide Enrichment and Mass Spectrometric Analysis

Protein (1 mg) was first reduced/alkylated and digested with Lys-C. The mixture was then diluted 4-fold to 2 M urea and digested further with trypsin. Strong cation exchange was performed as before (Pinkse et al., 2008); 24 fractions (1 min each, i.e., 50 μl elution volume) were collected by hand. The online TiO_2 chromatography was set using a triple stage precolumn, and both TiO_2 eluate and flowthrough fractions were chromatographically resolved using a 100 min linear gradient in the analytical column. The LTQ-Orbitrap was operated in data-dependent mode, automatically switching between MS and MS/MS. Full-scan MS spectra (m/z 400–1500) were acquired in the Orbitrap with a resolution of 60,000, and the two most intense ions were selected for MS/MS fragmentation in the linear ion trap. Further details can be found in the Supplemental Experimental Procedures.

Peptide Identification and Quantitative Analysis

Raw data were converted to single DTA files using Bioworks 3.2 and merged into Mascot Generic Format files, which were searched using an in-house licensed Mascot v2.2 search engine against IPI human 3.28 database (containing 68,020 sequences). Carbamidomethyl cysteine was set as fixed modification; protein N-acetylation, oxidized methionines, serine, threonine and tyrosine phosphorylation, deamidation, and SILAC-labels ([$^{13}C_6$,$^{15}N_4$]-arginine and [$^{13}C_6$,$^{15}N_2$]-lysine) were set as variable modifications. The mass tolerance of the precursor ion was 10 ppm and 0.9 Da for fragment ions. The false discovery rate was determined as < 1% (Mascot score threshold of 35) using the decoy database approach. MSQuant (http://msquant.sourceforge.net) was used to quantitate the levels of the identified phosphopeptides and determine the exact phosphorylation site within the peptide (Olsen et al., 2006). Every phosphopeptide quantitation was manually validated; peptides with low signal/noise ratios, low number of MS scans, or overlapping peaks were not included for quantitative purposes. StatQuant, an in-house-developed Java software, was used to correct for the arginine-to-proline conversion artifacts (Van Hoof et al., 2007), statistical analysis, comparison, and normalization.

Construction of Human SOX2 Mutants

Wild-type human *SOX2* was amplified by PCR using 5′-GGAATTCTCGGC GGCCGCCGGCGG-3′ in combination with 5′-GGAATTC*TCACAGATCCTC TTCTGAGATGAGTTTTGTTC*CATGTGTGAGAGGGGCAGTGTGC-3′ (EcoRI site, underlined; myc-tag sequence, italicized) and pcDNA3.1/Zeo-hSOX2 (a gift from Dr. N.A. Hanley) as template. The myc-tagged human *SOX2* PCR fragment was ligated into pGEM-T and sequenced to check for errors. Mutations were introduced by digestion of this pGEM-hSOX2-myc plasmid with *Bpl*I, followed by ligation of synthetic double-stranded oligos, outlined in Table S13, and sequencing to verify the mutations. Each human SOX2 construct was isolated from the different pGEM-hSOX2-myc variants by digestion with *EcoR*I and was ligated into pCAG-GFP-IRES-Puro^r (Braam et al., 2008) linearized using *EcoR*I, thus replacing the existing GFP open reading frame. The resulting pCAG-hSOX2-myc mutants were sequenced to confirm correct orientation behind the pCAG promoter.

Transfection and Immunofluorescent Analysis of HUES-7 Cells

HUES-7 cells were transfected as described previously (Braam et al., 2008) with the pCAG-hSOX2-myc variants and fixed after 48 hr. Fixed cells were stained using specific antibodies. For details, see Supplemental Experimental Procedures.

Culture and Transfection of HeLa Cells and Purification of His_6-SUMO2-Conjugated Proteins

HeLa cells, stably expressing His_6-SUMO2 were cultured as described previously (Vertegaal et al., 2004), and transfected with the pCAG-hSOX2-myc variants using polyethyleneimine. The following day, cells were lysed and His_6-SUMO2 conjugates purified on nickel-nitrilotriacetic acid-agarose beads (QIAGEN) as described previously (Schimmel et al., 2008).

SUPPLEMENTAL DATA

Supplemental Data include Supplemental Experimental Procedures, 13 figures, 13 tables, and 1 data set and can be found with this article online at http://www.cell.com/cell-stem-cell/supplemental/S1934-5909(09)00230-6.

ACKNOWLEDGMENTS

We thank Dr. A.C.O. Vertegaal for the nickel-nitrilotriacetic acid-agarose bead purification experiments; Dr. D. Melton for HUES-7; Dr. N.A. Hanley for pcDNA3.1/Zeo-hSox2; Dr. C. Denning for pCAG-GFP-IRES-Puro^r; Dr. M.J. Goumans for p-GSK3β and p-4EIFEBP1 antibodies; S. Mohammed for mass spectrometry support; and J. Gouw, B. van Breukelen, and H. van den Toorn for in-house software development. This work was supported by the Bsik programmes "Dutch Platform for Tissue Engineering," Stem Cells in Development and Disease; by the Netherlands Proteomic Center; by the FP6 EU Programme Heart Development and Heart Repair; and by the Netherlands Organisation for Scientific Research (NWO).

Received: November 19, 2008
Revised: March 31, 2009
Accepted: May 15, 2009
Published: August 6, 2009

REFERENCES

Adewumi, O., Aflatoonian, B., Ahrlund-Richter, L., Amit, M., Andrews, P.W., Beighton, G., Bello, P.A., Benvenisty, N., Berry, L.S., Bevan, S., et al. (2007). Characterization of human embryonic stem cell lines by the International Stem Cell Initiative. Nat. Biotechnol. *25*, 803–816.

Avilion, A.A., Nicolis, S.K., Pevny, L.H., Perez, L., Vivian, N., and Lovell-Badge, R. (2003). Multipotent cell lineages in early mouse development depend on SOX2 function. Genes Dev. *17*, 126–140.

Azuara, V., Perry, P., Sauer, S., Spivakov, M., Jorgensen, H.F., John, R.M., Gouti, M., Casanova, M., Warnes, G., Merkenschlager, M., et al. (2006). Chromatin signatures of pluripotent cell lines. Nat. Cell Biol. *8*, 532–538.

Barski, A., Cuddapah, S., Cui, K., Roh, T.Y., Schones, D.E., Wang, Z., Wei, G., Chepelev, I., and Zhao, K. (2007). High-resolution profiling of histone methylations in the human genome. Cell *129*, 823–837.

Bernstein, B.E., Mikkelsen, T.S., Xie, X., Kamal, M., Huebert, D.J., Cuff, J., Fry, B., Meissner, A., Wernig, M., Plath, K., et al. (2006). A bivalent chromatin structure marks key developmental genes in embryonic stem cells. Cell *125*, 315–326.

Binetruy, B., Heasley, L., Bost, F., Caron, L., and Aouadi, M. (2007). Concise review: regulation of embryonic stem cell lineage commitment by mitogen-activated protein kinases. Stem Cells *25*, 1090–1095.

Botuyan, M.V., Lee, J., Ward, I.M., Kim, J.E., Thompson, J.R., Chen, J., and Mer, G. (2006). Structural basis for the methylation state-specific recognition of histone H4-K20 by 53BP1 and Crb2 in DNA repair. Cell *127*, 1361–1373.

Boyer, L.A., Lee, T.I., Cole, M.F., Johnstone, S.E., Levine, S.S., Zucker, J.P., Guenther, M.G., Kumar, R.M., Murray, H.L., Jenner, R.G., et al. (2005). Core transcriptional regulatory circuitry in human embryonic stem cells. Cell *122*, 947–956.

Braam, S.R., Denning, C., van den Brink, S., Kats, P., Hochstenbach, R., Passier, R., and Mummery, C.L. (2008). Improved genetic manipulation of human embryonic stem cells. Nat. Methods *5*, 389–392.

Chambers, I., Silva, J., Colby, D., Nichols, J., Nijmeijer, B., Robertson, M., Vrana, J., Jones, K., Grotewold, L., and Smith, A. (2007). Nanog safeguards pluripotency and mediates germline development. Nature *450*, 1230–1234.

Chen, G., and Courey, A.J. (2000). Groucho/TLE family proteins and transcriptional repression. Gene *249*, 1–16.

Chew, J.L., Loh, Y.H., Zhang, W., Chen, X., Tam, W.L., Yeap, L.S., Li, P., Ang, Y.S., Lim, B., Robson, P., et al. (2005). Reciprocal transcriptional regulation of Pou5f1 and Sox2 via the Oct4/Sox2 complex in embryonic stem cells. Mol. Cell. Biol. *25*, 6031–6046.

Diella, F., Cameron, S., Gemund, C., Linding, R., Via, A., Kuster, B., Sicheritz-Ponten, T., Blom, N., and Gibson, T.J. (2004). Phospho.ELM: a database of experimentally verified phosphorylation sites in eukaryotic proteins. BMC Bioinformatics *5*, 79.

Eckert, J.J., and Fleming, T.P. (2008). Tight junction biogenesis during early development. Biochim. Biophys. Acta *1778*, 717–728.

Efroni, S., Duttagupta, R., Cheng, J., Dehghani, H., Hoeppner, D.J., Dash, C., Bazett-Jones, D.P., Le Grice, S., McKay, R.D., Buetow, K.H., et al. (2008). Global transcription in pluripotent embryonic stem cells. Cell Stem Cell *2*, 437–447.

Feldman, N., Gerson, A., Fang, J., Li, E., Zhang, Y., Shinkai, Y., Cedar, H., and Bergman, Y. (2006). G9a-mediated irreversible epigenetic inactivation of Oct-3/4 during early embryogenesis. Nat. Cell Biol. *8*, 188–194.

Fong, H., Hohenstein, K.A., and Donovan, P.J. (2008). Regulation of self-renewal and pluripotency by Sox2 in human embryonic stem cells. Stem Cells *26*, 1931–1938.

Freund, C., Ward-van Oostwaard, D., Monshouwer-Kloots, J., van den Brink, S., van Rooijen, M., Xu, X., Zweigerdt, R., Mummery, C., and Passier, R. (2008). Insulin redirects differentiation from cardiogenic mesoderm and endoderm to neuroectoderm in differentiating human embryonic stem cells. Stem Cells *26*, 724–733.

Fujita, J., Crane, A.M., Souza, M.K., Dejosez, M., Kyba, M., Flavell, R.A., Thomson, J.A., and Zwaka, T.P. (2008). Caspase activity mediates the differentiation of embryonic stem cells. Cell Stem Cell *2*, 595–601.

Gruhler, A., Olsen, J.V., Mohammed, S., Mortensen, P., Faergeman, N.J., Mann, M., and Jensen, O.N. (2005). Quantitative phosphoproteomics applied to the yeast pheromone signaling pathway. Mol. Cell. Proteomics *4*, 310–327.

Gu, Y., Rosenblatt, J., and Morgan, D.O. (1992). Cell cycle regulation of CDK2 activity by phosphorylation of Thr160 and Tyr15. EMBO J. *11*, 3995–4005.

Guenther, M.G., Levine, S.S., Boyer, L.A., Jaenisch, R., and Young, R.A. (2007). A chromatin landmark and transcription initiation at most promoters in human cells. Cell *130*, 77–88.

Gygi, S.P., Rochon, Y., Franza, B.R., and Aebersold, R. (1999). Correlation between protein and mRNA abundance in yeast. Mol. Cell. Biol. *19*, 1720–1730.

Hietakangas, V., Anckar, J., Blomster, H.A., Fujimoto, M., Palvimo, J.J., Nakai, A., and Sistonen, L. (2006). PDSM, a motif for phosphorylation-dependent SUMO modification. Proc. Natl. Acad. Sci. USA *103*, 45–50.

Irvine, K., Stirling, R., Hume, D., and Kennedy, D. (2004). Rasputin, more promiscuous than ever: a review of G3BP. Int. J. Dev. Biol. *48*, 1065–1077.

Jaenisch, R., and Young, R. (2008). Stem cells, the molecular circuitry of pluripotency and nuclear reprogramming. Cell *132*, 567–582.

Jelier, R., Schuemie, M.J., Veldhoven, A., Dorssers, L.C., Jenster, G., and Kors, J.A. (2008). Anni 2.0: a multipurpose text-mining tool for the life sciences. Genome Biol. *9*, R96.

Kopp, J.L., Ormsbee, B.D., Desler, M., and Rizzino, A. (2008). Small increases in the level of Sox2 trigger the differentiation of mouse embryonic stem cells. Stem Cells *26*, 903–911.

Kratchmarova, I., Blagoev, B., Haack-Sorensen, M., Kassem, M., and Mann, M. (2005). Mechanism of divergent growth factor effects in mesenchymal stem cell differentiation. Science *308*, 1472–1477.

Linding, R., Jensen, L.J., Ostheimer, G.J., van Vugt, M.A., Jorgensen, C., Miron, I.M., Diella, F., Colwill, K., Taylor, L., Elder, K., et al. (2007). Systematic discovery of in vivo phosphorylation networks. Cell *129*, 1415–1426.

Loh, Y.H., Wu, Q., Chew, J.L., Vega, V.B., Zhang, W., Chen, X., Bourque, G., George, J., Leong, B., Liu, J., et al. (2006). The Oct4 and Nanog transcription network regulates pluripotency in mouse embryonic stem cells. Nat. Genet. *38*, 431–440.

Manning, G., Whyte, D.B., Martinez, R., Hunter, T., and Sudarsanam, S. (2002). The protein kinase complement of the human genome. Science *298*, 1912–1934.

Marson, A., Levine, S.S., Cole, M.F., Frampton, G.M., Brambrink, T., Johnstone, S., Guenther, M.G., Johnston, W.K., Wernig, M., Newman, J.,

et al. (2008). Connecting microRNA genes to the core transcriptional regulatory circuitry of embryonic stem cells. Cell *134*, 521–533.

Masui, S., Nakatake, Y., Toyooka, Y., Shimosato, D., Yagi, R., Takahashi, K., Okochi, H., Okuda, A., Matoba, R., Sharov, A.A., et al. (2007). Pluripotency governed by Sox2 via regulation of Oct3/4 expression in mouse embryonic stem cells. Nat. Cell Biol. *9*, 625–635.

Mi, H., Guo, N., Kejariwal, A., and Thomas, P.D. (2007). PANTHER version 6: protein sequence and function evolution data with expanded representation of biological pathways. Nucleic Acids Res. *35*, D247–D252.

Mikkelsen, T.S., Ku, M., Jaffe, D.B., Issac, B., Lieberman, E., Giannoukos, G., Alvarez, P., Brockman, W., Kim, T.K., Koche, R.P., et al. (2007). Genome-wide maps of chromatin state in pluripotent and lineage-committed cells. Nature *448*, 553–560.

Miller-Jensen, K., Janes, K.A., Brugge, J.S., and Lauffenburger, D.A. (2007). Common effector processing mediates cell-specific responses to stimuli. Nature *448*, 604–608.

Mitsui, K., Tokuzawa, Y., Itoh, H., Segawa, K., Murakami, M., Takahashi, K., Maruyama, M., Maeda, M., and Yamanaka, S. (2003). The homeoprotein Nanog is required for maintenance of pluripotency in mouse epiblast and ES cells. Cell *113*, 631–642.

Muller, F.J., Laurent, L.C., Kostka, D., Ulitsky, I., Williams, R., Lu, C., Park, I.H., Rao, M.S., Shamir, R., Schwartz, P.H., et al. (2008). Regulatory networks define phenotypic classes of human stem cell lines. Nature *455*, 401–405.

Niwa, H., Miyazaki, J., and Smith, A.G. (2000). Quantitative expression of Oct-3/4 defines differentiation, dedifferentiation or self-renewal of ES cells. Nat. Genet. *24*, 372–376.

Olsen, J.V., Blagoev, B., Gnad, F., Macek, B., Kumar, C., Mortensen, P., and Mann, M. (2006). Global, in vivo, and site-specific phosphorylation dynamics in signaling networks. Cell *127*, 635–648.

Ong, S.E., Blagoev, B., Kratchmarova, I., Kristensen, D.B., Steen, H., Pandey, A., and Mann, M. (2002). Stable isotope labeling by amino acids in cell culture, SILAC, as a simple and accurate approach to expression proteomics. Mol. Cell. Proteomics *1*, 376–386.

Pan, G., Tian, S., Nie, J., Yang, C., Ruotti, V., Wei, H., Jonsdottir, G.A., Stewart, R., and Thomson, J.A. (2007). Whole-genome analysis of histone H3 lysine 4 and lysine 27 methylation in human embryonic stem cells. Cell Stem Cell *1*, 299–312.

Pera, M.F., Andrade, J., Houssami, S., Reubinoff, B., Trounson, A., Stanley, E.G., Ward-van Oostwaard, D., and Mummery, C. (2004). Regulation of human embryonic stem cell differentiation by BMP-2 and its antagonist noggin. J. Cell Sci. *117*, 1269–1280.

Pinkse, M.W., Mohammed, S., Gouw, J.W., van Breukelen, B., Vos, H.R., and Heck, A.J. (2008). Highly robust, automated, and sensitive online TiO2-based phosphoproteomics applied to study endogenous phosphorylation in Drosophila melanogaster. J. Proteome Res. *7*, 687–697.

Sampath, P., Pritchard, D.K., Pabon, L., Reinecke, H., Schwartz, S.M., Morris, D.R., and Murry, C.E. (2008). A hierarchical network controls protein translation during murine embryonic stem cell self-renewal and differentiation. Cell Stem Cell *2*, 448–460.

Schimmel, J., Larsen, K.M., Matic, I., van Hagen, M., Cox, J., Mann, M., Andersen, J.S., and Vertegaal, A.C. (2008). The ubiquitin-proteasome system is a key component of the SUMO-2/3 cycle. Mol. Cell. Proteomics *7*, 2107–2122.

Shao, Z., Bhattacharya, K., Hsich, E., Park, L., Walters, B., Germann, U., Wang, Y.M., Kyriakis, J., Mohanlal, R., Kuida, K., et al. (2006). c-Jun N-terminal kinases mediate reactivation of Akt and cardiomyocyte survival after hypoxic injury in vitro and in vivo. Circ. Res. *98*, 111–118.

Thomson, J.A., Itskovitz-Eldor, J., Shapiro, S.S., Waknitz, M.A., Swiergiel, J.J., Marshall, V.S., and Jones, J.M. (1998). Embryonic stem cell lines derived from human blastocysts. Science *282*, 1145–1147.

Tsuruzoe, S., Ishihara, K., Uchimura, Y., Watanabe, S., Sekita, Y., Aoto, T., Saitoh, H., Yuasa, Y., Niwa, H., Kawasuji, M., et al. (2006). Inhibition of DNA binding of Sox2 by the SUMO conjugation. Biochem. Biophys. Res. Commun. *351*, 920–926.

Vallier, L., Alexander, M., and Pedersen, R.A. (2005). Activin/Nodal and FGF pathways cooperate to maintain pluripotency of human embryonic stem cells. J. Cell Sci. *118*, 4495–4509.

van den Boom, V., Kooistra, S.M., Boesjes, M., Geverts, B., Houtsmuller, A.B., Monzen, K., Komuro, I., Essers, J., Drenth-Diephuis, L.J., and Eggen, B.J. (2007). UTF1 is a chromatin-associated protein involved in ES cell differentiation. J. Cell Biol. *178*, 913–924.

Van Hoof, D., Passier, R., Ward-Van Oostwaard, D., Pinkse, M.W., Heck, A.J., Mummery, C.L., and Krijgsveld, J. (2006). A quest for human and mouse embryonic stem cell-specific proteins. Mol. Cell. Proteomics *5*, 1261–1273.

Van Hoof, D., Pinkse, M.W., Oostwaard, D.W., Mummery, C.L., Heck, A.J., and Krijgsveld, J. (2007). An experimental correction for arginine-to-proline conversion artifacts in SILAC-based quantitative proteomics. Nat. Methods *4*, 677–678.

Van Hoof, D., Braam, S.R., Dormeyer, W., Ward-van Oostwaard, D., Heck, A.J., Krijgsveld, J., and Mummery, C.L. (2008). Feeder-free monolayer cultures of human embryonic stem cells express an epithelial plasma membrane protein profile. Stem Cells *26*, 2777–2781.

Vertegaal, A.C., Ogg, S.C., Jaffray, E., Rodriguez, M.S., Hay, R.T., Andersen, J.S., Mann, M., and Lamond, A.I. (2004). A proteomic study of SUMO-2 target proteins. J. Biol. Chem. *279*, 33791–33798.

Vertegaal, A.C., Andersen, J.S., Ogg, S.C., Hay, R.T., Mann, M., and Lamond, A.I. (2006). Distinct and overlapping sets of SUMO-1 and SUMO-2 target proteins revealed by quantitative proteomics. Mol. Cell. Proteomics *5*, 2298–2310.

Viswanathan, S.R., Daley, G.Q., and Gregory, R.I. (2008). Selective blockade of microRNA processing by Lin28. Science *320*, 97–100.

Xu, R.H., Chen, X., Li, D.S., Li, R., Addicks, G.C., Glennon, C., Zwaka, T.P., and Thomson, J.A. (2002). BMP4 initiates human embryonic stem cell differentiation to trophoblast. Nat. Biotechnol. *20*, 1261–1264.

Xu, R.H., Peck, R.M., Li, D.S., Feng, X., Ludwig, T., and Thomson, J.A. (2005). Basic FGF and suppression of BMP signaling sustain undifferentiated proliferation of human ES cells. Nat. Methods *2*, 185–190.

Xu, R.H., Sampsell-Barron, T.L., Gu, F., Root, S., Peck, R.M., Pan, G., Yu, J., Antosiewicz-Bourget, J., Tian, S., Stewart, R., et al. (2008). NANOG is a direct target of TGFbeta/activin-mediated SMAD signaling in human ESCs. Cell Stem Cell *3*, 196–206.

Ying, Q.L., Nichols, J., Chambers, I., and Smith, A. (2003). BMP induction of Id proteins suppresses differentiation and sustains embryonic stem cell self-renewal in collaboration with STAT3. Cell *115*, 281–292.

Yu, J., Vodyanik, M.A., Smuga-Otto, K., Antosiewicz-Bourget, J., Frane, J.L., Tian, S., Nie, J., Jonsdottir, G.A., Ruotti, V., Stewart, R., et al. (2007). Induced pluripotent stem cell lines derived from human somatic cells. Science *318*, 1917–1920.

Yuan, H., Corbi, N., Basilico, C., and Dailey, L. (1995). Developmental-specific activity of the FGF-4 enhancer requires the synergistic action of Sox2 and Oct-3. Genes Dev. *9*, 2635–2645.